Unique parameter identification for model-based cardiac diagnosis in critical care

Christopher. E. Hann*, J. Geoffrey Chase*, Thomas Desaive, Claire F. Froissart***, James Revie*, David Stevenson*, Bernard Lambermont**, Alexandre Ghuysen**, Philippe Kolh** and Geoffrey M. Shaw ****

**Mechanical Eng, Centre for Bio-Engineering, University of Canterbury, Christchurch, New Zealand (Tel: +64-3-364-7001; e-mail: Chris.Hann@canterbury.ac.nz).*
***Hemodynamics Research Laboratory, University of Liege, Belgium (e-mail: tdesaive@ulg.ac.be)*
****Université de Technologie de Belfort-Montbéliard, France*
*****Department of Intensive Care, Christchurch Hospital, Christchurch, New Zealand*

Abstract: Lumped parameter approaches for modeling the cardiovascular system typically have many parameters of which many are not identifiable. The conventional approach is to only identify a small subset of parameters to match measured data, and to set the remaining parameters at population values. These values are often based on animal data or the "average human" response. The problem, is that setting many parameters at nominal fixed values, may introduce dynamics that are not present in a specific patient. As parameter numbers and model complexity increase, more clinical data is required for validation and the model limitations are harder to quantify. This paper considers the modeling and the parameter identification simultaneously, and creates models that are one to one with the measurements. That is, every input parameter into the model is uniquely optimized to capture the clinical data and no parameters are set at population values. The result is a geometrical characterization of a previously developed six chamber heart model, and a completely patient specific approach to cardiac diagnosis in critical care. In addition, simplified sub-structures of the six chamber model are created to provide very fast and accurate parameter identification from arbitrary starting points and with no prior knowledge on the parameters. Furthermore, by utilizing continuous information from the arterial/pulmonary pressure waveforms and the end-diastolic time, it is shown that only the stroke volumes of the ventricles are required for adequate cardiac diagnosis. This reduced data set is more practical for an intensive care unit as the maximum and minimum volumes are no longer needed, which was a requirement in prior work. The simplified models can also act as a bridge to identifying more sophisticated cardiac models, by providing a generating set of waveforms that the complex models can match to. Most importantly, this approach does not have any predefined assumptions on patient dynamics other than the basic model structure, and is thus suitable for improving cardiovascular management in critical care by optimizing therapy for individual patients.

1. INTRODUCTION

In critical care, cardiovascular dysfunction can be easily misdiagnosed due to the array of sometimes conflicting data The overall goal of this research is to use computational cardiac models to better aggregate available clinical data in an intensive care unit (ICU) into a more readily understood physiological context for clinicians. The computational models can be used to reveal dynamics and interactions non-obviously hidden in the data, enabling simpler and more robust diagnosis.

A major difficulty faced with cardiovascular modelling is the level of detail these models typically include. For example multi-scale modelling approaches utilizing finite elements have successfully explained complex behaviour of the heart [Kerckhoffs 2007]. However, a large gap exists between the computational results of these detailed models and clinical utility.

This paper presents a different approach, by first developing simplified, fully identifiable, patient specific models, that are based around the clinical data available in an ICU. These models can serve as a bridge to identify more complicated and physiologically accurate models as required to predict the observed patient hemodynamic responses. In the simplified models, patient specific dynamics are only considered if they can be uniquely identified from the given data. Due to the simplified structure of these models, it is then possible to analyze individual geometric effects of given input parameters on the output. This information will lead to the minimal set of features in the outputs, that are required for adequate cardiac diagnosis.

The starting baseline model structure considered is a six chamber cardiovascular system (CVS) model including

ventricular interaction and inertial effects that has been previously developed [Smith et al 2004] and validated in clinical animal trials [Starfinger 2007, Starfinger 2008]. However, note that the approach is general and could be applied to any cardiac model structure.

A new concept developed in this paper matches simplified CVS model outputs to continuous information of arterial/pulmonary pressures and the end-diastolic time from an electrocardiogram (ECG) or the "a wave" timing from the pulmonary pressure waveform. Adding continuous pressure waveforms and end-diastolic timing to current clinical data sets is shown to increase the diagnostic ability of the model and enable a more minimal data set that doesn't require maximum and minimum volume measurements. Hence, this approach adds a simple and easy measurement to remove the need for a more invasive, difficult and noisy measurement. New methods are rigorously tested in simulation with noise corrupted measurements and modelling error to prove robustness. Finally, animal data is used to demonstrate the clinical potential of these methods.

2. METHODS

2.1 Simplified cardiac models

The baseline cardiovascular system model used in this paper consists of six elastic chambers [Smith 2004, Hann 2005]. The parameters P_{pu}, and P_{vc} in the model are essentially close to constant. Hence, if P_{pu}, and P_{vc} are constant for the model of Figure 1, and ventricular interaction V_{spt} and the pressure in the pericardium P_{pcd} are set to zero, both the left and right systems of the CVS can be separated. However, note that by identifying both systems to measured data, there is still an inherent coupling by the fact that the stroke volumes of the left and right ventricles would be the same. A further simplification is to set L_{mt}, L_{av} and $P_{0,lvf}$ to 0. The resulting two models are shown in Figure 1.

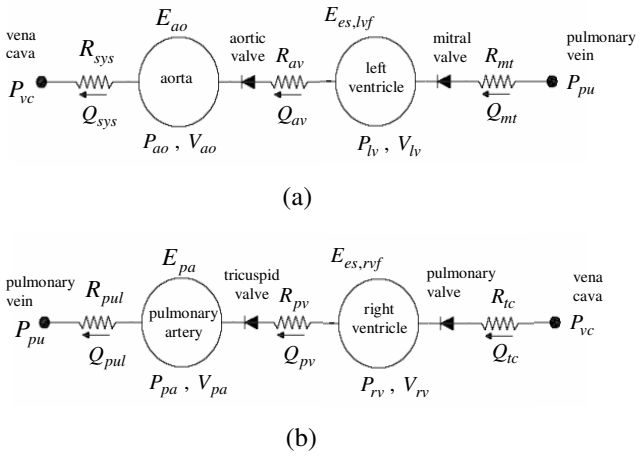

Fig. 1: (a) The left ventricle-systemic system simplified model (b) The right ventricle-pulmonary system simplified model

Replacing the input/output parameters

$$\text{LV Input parameters} \equiv \left\{P_{pu}, E_{es,lvf}, E_{ao}, R_{mt}, R_{av}, R_{sys}, P_{vc}\right\} \quad (1)$$

$$\text{LV Output parameters} \equiv \left\{Q_{mt}, P_{lv}, V_{lv}, Q_{av}, P_{ao}, Q_{sys}\right\} \quad (2)$$

in the left ventricle-systemic system of Figure 2(a) with the parameters :

$$\text{RV Input parameters} \equiv \left\{P_{vc}, E_{es,rvf}, E_{pa}, R_{tc}, R_{pv}, R_{pul}, P_{pu}\right\} \quad (3)$$

$$\text{RV Output parameters} \equiv \left\{Q_{tc}, P_{rv}, V_{rv}, Q_{pv}, P_{pa}, Q_{pul}\right\} \quad (4)$$

the right ventricle-pulmonary model of Figure 1(b) is obtained.

A final addition is to create an extended driver function *e(t)* to reduce the modelling error caused by the above simplified model assumptions. The new driver function and the model differential equations for the left ventricle-systemic system of Figure 1(a) are defined:

$$\dot{V}_{lv} = H(Q_{mt})Q_{mt} - H(Q_{av})Q_{av} \quad (5)$$

$$\dot{P}_{ao} = E_{ao}H(Q_{av})Q_{av} - E_{ao}\left(\frac{P_{ao} - P_{vc}}{R_{sys}}\right) \quad (6)$$

$$Q_{mt} = \frac{P_{pu} - P_{lv}}{R_{mt}} \quad (7)$$

$$Q_{av} = \frac{P_{lv} - P_{ao}}{R_{av}} \quad (8)$$

$$P_{lv} = e(t)E_{es,lvf}V_{lv} + P_{th} \quad (9)$$

$$e_{new}(t) = \frac{P_{lv,full} - P_{th}}{V_{lv,full}} \quad (10)$$

where $H(Q)$ is the Heaviside function. The parameters $P_{lv,full}$ and $V_{lv,full}$ are defined to be the full model outputs from a healthy human parameter set with a heart beat period of 0.75 seconds [Hann 2005]. Hence Equation (10) represents a population driver function, which could be scaled to represent different heart beats, and the shape altered as required to capture individual patients.

2.3 Healthy and disease state comparisons

This paper concentrates on the left ventricle-systemic system of Figure 1(a) to demonstrate the methods, but the symmetry between Figures 1(a) and (b) ensures the same methods will equally apply to the right side. To obtain a diseased human the following set of parameter changes are made [Smith 2007]:

$$R_{av} \to 4R_{av},\ R_{mt} \to 4R_{mt},\ E_{es,lvf} \to \frac{1}{2}E_{es,lvf},\ R_{sys} \to \frac{1}{2}R_{sys} \quad (11)$$

The changes in Equation (11) are used as an initial mathematical validation of the simplified models in Figure 1.

2.4 Parameter identification

The unknown patient specific parameters, denoted X, that are optimized for the left ventricle are defined:

$$X \equiv \left\{ P_{pu}, E_{es,lvf}, E_{ao}, R_{mt}, R_{av}, R_{sys} \right\} \tag{12}$$

where P_{vc} can be found from identifying the right ventricle system, or by direct measurement, which is commonly done.

The measured maximum/minimum left ventricle volume and aortic pressure can only uniquely identify 4 of the parameters of Equation (12). However, the timing of the mitral valve closure corresponds to the end of atrial contraction which can be detected by the end of the P wave on an electrocardiogram (ECG). Alternatively, since the left and right atriums contract close to simultaneously, the mitral valve closure can also be calculated from the "a wave" in the pulmonary artery and/or the central venous pressure waveform.

These observations demonstrate an important concept, which is to utilize features from physiological waveforms to improve identifiability without having to explicitly model the effects. The pressure in the pulmonary vein P_{pu} or the filling pressure of the simplified model of Figure 1(a) corresponds to the left ventricle pressure at the mitral valve closure. Hence, P_{pu} can be estimated by the formula:

$$P_{pu} = P_{lv}(t_{d2}), \quad t_{d2} \equiv \text{time of mitral valve closure} \tag{13}$$

Note that another alternative is to indirectly infer the filling pressure from the height of the "a wave" in the pulmonary artery which has been shown in studies to have high correlations of 0.93. However, the method of Equation (13) is used in this paper as it is more direct.

A further important feature available is the maximum gradient or inflection point in the ascending aortic pressure wave. The parameter which has a significant effect on the maximum aortic pressure gradient is the resistance in the aortic valve R_{av}. Define:

$$\alpha(R_{av}) = \frac{P_{ao,approx}(t_{inflect}) - P_{ao,approx}(t_{min})}{P_{ao,true}(t_{inflect}) - P_{ao,true}(t_{min})} \, R_{av,old} \tag{14}$$

where $P_{ao,approx}$ and $P_{ao,true}$ are the simulated and "measured" aortic pressures, t_{min} is the time of minimum aortic pressure and $t_{inflect}$ is the time of maximum aortic pressure gradient. Equation (14) is an approximation to the ratio of the maximum gradients of $P_{ao,approx}$ to $P_{ao,true}$ and is used to avoid having to differentiate the aortic pressure. If R_{av} increases by a factor of 2, with all other parameters fixed, α approximately reduces by a factor of 2, with a much less effect on the maximum and minimum volumes/pressures. This result motivates an approximation to R_{av}:

$$R_{av,approx} = \frac{P_{ao,true}(t_{inflect}) - P_{ao,true}(t_{min})}{P_{ao,approx}(t_{inflect}) - P_{ao,approx}(t_{min})} \tag{15}$$

However, for Equation (13) and (15) to be valid the approximations $P_{lv,approx}$ and $P_{ao,approx}$ need to be as accurate as possible. The solution proposed, is to first ensure that the maximum/minimum simulated volumes and aortic pressures are precisely matched to the measured values for given initial (but essentially arbitrary) estimates of P_{pu} and R_{av}. At the end of this optimization, P_{pu} and R_{av} are updated using Equations (13) and (14).

Increasing $E_{es,lvf}$, R_{mt}, E_{ao} and R_{sys} separately by factors of 2, decrease the mean volume and stroke volume and increase the pulse pressure difference (PP) and mean aortic pressure. These results motivate the following definitions:

$$E_{es,lvf,approx} = \left(\frac{V_{lv,min,true} + V_{lv,max,true}}{V_{lv,min,approx} + V_{lv,max,approx}} \right) E_{es,lvf,old} \tag{16}$$

$$R_{mt,approx} = \left(\frac{SV_{true}}{SV_{approx}} \right) R_{mt,old} \tag{17}$$

$$E_{ao,approx} = \left(\frac{PP_{true}}{PP_{approx}} \right) E_{ao,old} \tag{18}$$

$$R_{sys,approx} = \left(\frac{P_{ao,max,true} + P_{ao,min,true}}{P_{ao,max,approx} + P_{ao,min,approx}} \right) R_{sys,old} \tag{19}$$

Note that Equations (16)-(19) can also be inferred with the appropriate approximations, from an integral formulation of Equations (5)-(9) over one heart beat (details not shown). This process is similar to the concept used in prior work [Hann 2006, Starfinger 2007], but a fundamental difference is that the updated approximations in Equations (16)-(19) do not require estimates of the continuous waveform V_{lv} which is not typically known. Equations (16)-(19) are similar to proportional feedback control, which doesn't require a predetermined waveform shape and is fully automatic. The parameter identification method is summarized in Figure 2.

Step1 Choose arbitrary set of input parameters including P_{pu} and R_{av}

Step2 Simulate model of Equations (5)-(10)

Step3 Compute approximations to $E_{es,lvf}$, R_{mt}, E_{ao} and R_{sys} from Equations (16)-(19).

Step4 Simulate model Equations (5)-(10).

Step5 If the maximum volumes and aortic pressures are matched within a given tolerance go to Step6, otherwise go back to Step3.

Step6 Compute P_{pu} and R_{av} from Equations (13) and (15). If they have changed by less than 1% go to Step7 otherwise go back to Step3.

Step7 Output final solution and identified parameters

Fig. 2: Parameter identification algorithm for Figure 1(a)

3. RESULTS AND DISCUSSION

Measurement error is simulated by corrupting the simulated data with random uniformly distributed noise. Due to the

symmetry of Figures 1(a) and (b) only tests on the left-ventricle system are considered. The noise is defined:

$$\text{uniform noise} \equiv 5\% \text{ in } P_{ao}(t), 10\% \text{ in SV} \quad (20)$$

Note that the specific noise model used is effectively arbitrary, since it is the magnitude of the noise which has the largest effect on results. However, the assumption of uniformity is a conservative test where outliers are more likely to occur. The noise is made less for the pressure, since it is assumed that a catheter measures the aortic pressure waveform, which is more accurate and standard in an ICU.

3.1 Healthy human – no noise

The parameter identification method of Figure 2 is tested using the simulated healthy human with input and output parameters defined in [Hann 2005]. For this example no random noise is added. The assumed measured data is:

$$\text{measured data} \equiv \text{mean } V_{lv}, SV, PP, \text{mean } P_{ao}, P_{ao}(t), t_{d2} \quad (21)$$

where P_{ao} is given as a function of time since it is continuously measured. Figure 2 is now applied to the healthy human data of Equation (21). The left ventricle volume matches very closely to the true volume with maximum errors of 1.6% and 2.6% during filling and ejection. Similarly small errors less than 2% are observed in the aortic pressure. The error in the maximum ventricle pressure is 2.1%. The parameters are identified with errors typically less than 10% except an error of 21% in R_{av} which is largely due to its small value. These accurate results provide an initial validation of the parameter identification method of Figure 2.

In addition, very fast convergence is obtained even when starting significantly far away from the solution. For example starting with an initial guess of parameters with 300-400% error in all the parameters, takes approximately 24 iterations (or model simulations) for the parameters to converge within 1%. This convergence time can be reduced by a factor of 2 by re-defining R_{av} in Equation (15) by:

$$R_{av,approx} = \left(\frac{P_{ao,true}(t_{inflect}) - P_{ao,true}(t_{min})}{P_{ao,approx}(t_{inflect}) - P_{ao,approx}(t_{min})} \right)^{\text{gain}} R_{av} \quad (22)$$

and setting a gain of 3. Importantly, once the method converges, this implies that the ratios in Equations (16)-(19) must be unity, otherwise the parameters would keep changing. Hence, the method can never reach a local minima and must always stop at the global minimum.

3.2 Diseased human – no noise

The algorithm of Figure 2 is now applied to a diseased human which is defined to be the output of the full six chamber model using the parameters of Equation (11). Again the measured data is taken to be the output parameters in Equation (21), but no noise is applied. The results (not shown) again show very accurate identification of the disease state, and further confirm the validity of the simplified models of Figure 1 to approximate the six chamber model.

3.3 Healthy/Diseased human – noise and no mean V_{lv}

Noise is now added to the measurements and the mean volume measurement of Equation (21) is removed and made an unknown parameter to optimize. To account for the increase in unknown parameters, more information from the aortic pressure waveform is used. Define:

$$error(\text{mean } V_{lv}) = \sqrt{\sum_{i=1}^{n} (P_{ao,approx}(t_i) - P_{ao,true}(t_i))^2} \quad (23)$$

$$t_1 = t_{min}, \; t_n = t_{min} + 3(t_{inflect} - t_{min})$$
$$n \equiv \#\text{equally spaced time points} \in [t_1, t_n] \quad (24)$$

where t_{min} and $t_{inflect}$ are from Equation (15), and n is dependent on the sampling frequency of the aortic pressure catheter which is taken to be 1kHz. The metric *error* is dependent on the mean V_{lv} and the points t_1 and t_n are equally spaced about $t_{inflect}$. It is important to note that the full aortic pressure waveform cannot be used in Equation (23). The reason is that the model does not capture the diacrotic notch so matching to this part of the waveform would introduce unnecessary error into the method. However, the continuous waveform in the interval [t_1, t_n] still provides significantly extra data that can be used to identify the mean volume and thus the maximum/minimum left ventricle volumes as well. The method is based around a line search about the parameter $V_{lv,max}$ = mean V_{lv}+SV/2. Define:

$$V_{lv,max,approx} = \{\max V_{lv}(X) \mid error(\text{mean } V_{lv}) \text{ is minimal}\} \quad (25)$$

where *error*(mean V_{lv}) is defined in Equation (23). The combination of Equation (25) and Figure 2 presents the final parameter identification method.

100 Monte Carlo simulations are performed for the algorithm of Figure 2 and Equation (25) with noise levels defined in Equation (20). To optimize accuracy, a cubic smoothing spline is performed on the noisy aortic pressure waveform using standard in-built functions in Matlab. The identified parameters are summarized in Table 1:

Parameters	Healthy		Diseased	
	Median	90% CI	Median	90% CI
P_{pu}	1.7	[0.8,3.0]	3.7	[1.2,7]
R_{av}	0.012	[0.006,0.02]	0.064	[0.038,0.082]
$E_{es,lvf}$	2.3	[2.0,2.8]	1.1	[0.9,1.3]
R_{mt}	0.015	[0.01,0.02]	0.06	[0.042,0.09]
R_{sys}	1.10	[1.00,1.20]	0.53	[0.49,0.58]
E_{ao}	0.70	[0.64,0.75]	0.68	[0.62,0.75]

Table 1: Comparing the identified parameters for a healthy and diseased human with noise from Equation (20).

In Table 1, there are significant separations in the 90% CI's except for P_{pu} which doesn't increase much without noise. For the healthy and disease states, 90% of the identified volume have errors less than 8.7% and 11.5% and 90% of the identified maximum left ventricle pressures have errors less than 1.5% and 9.4%.

3.4 Validation on an animal model and clinical implementation.

To demonstrate the clinical potential for the methods developed, data from a porcine pulmonary embolism experiment is used. The data is obtained from the Hemodynamics Research Laboratory, University of Liege, Belgium. In the experiments, a pig is injected with autologous blood clots every two hours to simulate pulmonary embolism [Ghuysen 2007].

As a simple proof of concept, the left ventricle model of Figure 1(a) and the method of Figure 2 are applied using measured waveforms for one of the pigs at two time points of 30 minutes and 210 minutes. A driver function is derived in a similar way to Equation (10), but with $P_{lv,full}$ and $V_{lv,full}$ replaced by the measured left ventricle pressure and volume, and P_{th} is set to 0, since the pig is open chest. The resulting function is smoothed by least squares cubic splines and normalized so the maximum point is 1 and the time interval of one heart beat is the healthy value of 0.75. To account for different heart rates, the generic shape is defined:

$$\hat{e}(t) = \bar{e}\left(\frac{0.75}{period}t\right) \tag{26}$$

where $\bar{e}(t)$ is experimentally derived from the healthy state of several pigs based on an average response. The final driver function is defined:

$$e(t) = \hat{e}(\alpha t + \beta), \quad 0 < t < period$$
$$\alpha = \frac{t_{\nabla ao,min} - t_{ao,min}}{t_{inflect,2} - t_{inflect,1}}, \beta = \frac{t_{ao,min}t_{inflect,2} - t_{\nabla ao,min}t_{inflect,1}}{t_{inflect,2} - t_{inflect,1}} \tag{27}$$

where $t_{ao,min}$ is the time of minimum aortic pressure, $t_{\nabla ao,min}$ is the time of the minimum aortic pressure gradient, and $t_{inflect,1}$ and $t_{inflect,2}$ are the first and second inflection points of $\hat{e}$ in Equation (26). Specifically, $t_{\nabla ao,min}$ is well known to correspond to the minimum left ventricle pressure gradient (or inflection point) which always occurs just before the diacrotic notch, and thus corresponds to the aortic valve closure. The volume is approximately constant at this point, and therefore, the formula of Equation (10) shows that $t_{inflect,2}$ should be equal to $t_{\nabla ao,min}$. The maximum left ventricle pressure gradient, is also known to occur just before the aortic valve opens, which corresponds closely to $t_{ao,min}$. Therefore since the volume is constant at this point as well, $t_{inflect,1}$ should be equal to $t_{ao,min}$. The time scaling transformation in Equation (27) ensures that the inflection points of the driver function correspond to $t_{ao,min}$ and $t_{\nabla ao,min}$ as required. Equations (26) and (27) therefore provide a way of approximately identifying a patient (pig) specific driver function. Note that in an ICU setting, depending on the different heart failure types, there would be large variations in the shape of the driver functions. However, the definition of Equations (26) and (27) approximately accounts for variations by scaling the main features (inflection points) to match the measured physiological response (arterial pressure waveform). The ascending aortic pressure waveform is also known to mimic the ascending left ventricular pressure so could also help to approximate the driver function, but is left to future work.

3.4.1 Parameter identification with known volumes

Figure 3(a) shows the result of applying the algorithm of Figure 2 on the one of the pigs at 30 minutes into the pulmonary embolism experiment. For comparison, the values of P_{pu}=2 and R_{av}=0.46 are chosen for step 1 in the algorithm of Figure 2, and only steps 2-5 are performed to match the data. The result is given in Figure 3(b). In both cases the maximum and minimum values of V_{lv} and P_{ao} (not shown) are accurately captured, but there are errors of 34% and 84% in the parameters $E_{es,lvf}$ and R_{mt}. The errors in E_{ao} and R_{sys} are less than 5%. However, the parameter $E_{es,lvf}$ appears relatively robust and is virtually unaffected by changes in P_{pu}. For example if R_{av}<0.2, the errors of $E_{es,lvf}$ are less than 10%. But these results highlight the importance of the data set in Equation (21) to accurately identify the model as well as finding a unique parameter set.

The PV curve and aortic pressure waveform corresponding to the correct parameters in Figure 3(a) are plotted in Figure 4, showing a close match. Notice how the first third to a half of the ascending aortic pressure is matched almost exactly. The high degree of accuracy in this period is due to the parameter identification method forcing the inflection point of the model to match the inflection point of the data. This result further shows the power of the method of Figure 2 as any feature that the model of Figure 1(a) is capable of matching, can be precisely captured independent of starting point, with very fast convergence and very minimal computation.

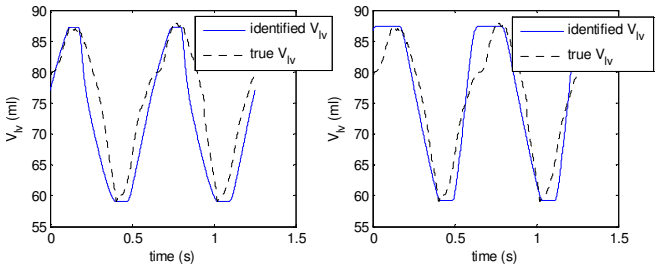

Fig. 3: Applying the algorithm of Figure 2 to the pig data. (a) identifying all parameters (b) fixing P_{pu} and R_{av}

It has been shown that the ascending aortic waveform inflection point is a predictive factor for all-cause and cardiovascular mortality in patients with chronic renal failure on hemodialysis [Ueda 2004]. Many other studies have also

shown features in the continuous aortic pressure waveform to help diagnose disease states and to monitor improvements due to therapy. Therefore, this modelling and parameter identification approach has the potential to aggregate key clinical information and any significant correlations between parameters observed in the literature.

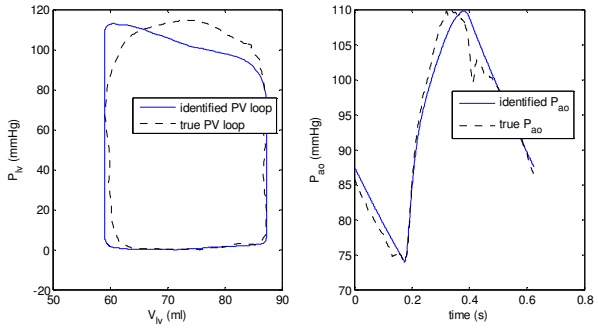

Fig 4: Identification results using correct parameters of Fig. 3(a). (a) Pressure-volume curve (b) Aortic pressure waveform

3.4.2 Parameter identification with mean V_{lv} unknown

The method with mean V_{lv} as an extra unknown, is applied on two separate time periods, at 30 minutes and 120 minutes. The results of the identified parameters are compared to the parameters identified in Figures 3(b) and 4, which are treated as the "true" parameters. For the pig at 30 minutes, the method identified R_{mt}, R_{sys}, E_{ao} and P_{pu} with an accuracy less than 3% of the true values, with errors of 7.6% in $E_{es,lvf}$ and 18.8% in R_{av}. However the larger error in R_{av} can be attributed to the small size of the true value for R_{av}. The errors for the identified left ventricle volume and pressure were 4.6% and 1.0%. For the pig at 120 minutes, the method identified R_{mt}, R_{sys}, E_{ao} and P_{pu} with an accuracy less than 2% of the true values, with errors of 5.1% in $E_{es,lvf}$ and 14.7% in R_{av}. These results combined with the simulated results in the prior section suggest that the volume may not be needed to identify parameters, but requires further validation in clinical trials which are planned.

4. CONCLUSIONS

Two simplified models for the left-ventricle systemic and right-ventricle pulmonary systems were developed. These models captured closely simulated outputs from a more complex six chamber model, and were shown to be uniquely identifiable with the addition of the end-diastolic filling time and continuous information from the aortic pressure waveform. Furthermore, the extra data used, that is readily available in an ICU, enabled the mean volume to be added as an extra unknown parameter with minimal effect on identifiability. This result has significant potential clinically, as the maximum/minimum volumes are hard to measure, where stroke volume is relatively easy and more common.

The approach of breaking down the six chamber heart model into separate uniquely identifiable models is general and could be applied to any lumped parameter CVS model. In particular, future work will utilize the simpler models to allow rapid identification of the 8 chamber model [Starfinger 2008] and any other added dynamics as required to diagnose cardiac disease states and characterize therapy response.

The methods were successfully tested in simulation with noise and on animal data using available data. The results require further validation on other disease states, but show potential for eventual clinical implementation of a model-based cardiac diagnosis/therapeutics system in the ICU.

REFERENCES

Kerckhoffs, RCP, Neal, ML, Gu, Q, Bassingthwaighte, JB, Omens, JH and McCulloch, AD. "Coupling of a 3D finite element model of cardiac ventricular mechanics to lumped systems of the systemic and pulmonic circulation," Ann. Biomed. Eng., Vol 35, pp. 1-18, 2007.

Smith, BW, Chase, JG, Nokes, RI, Shaw, GM and Wake, G. "Minimal haemodynamic system model including ventricular interaction and valve dynamics," Med. Eng. Phys, Vol 26, pp.131-139, 2004.

Starfinger C, Hann, CE, Chase, JG, Desaive T, Ghuysen A and Shaw, G. "Model-based Cardiac Diagnosis of Pulmonary Embolism," Computer Methods and Programs in Biomedicine, Vol 87(1): pp. 46-60, 2007.

Starfinger, C, Chase, JG, Hann, CE, Shaw, GM, Lambermont, B, Ghuysen, A, Kolh, P, Dauby, PC and Desaive, T. "Model-based identification and diagnosis of a porcine model of induced endotoxic shock with hemofiltration," Mathematical Biosciences, Vol 216(2), pp. 132-139, 2008a.

Hann, CE, Chase, JG and Shaw, GM, "Efficient implementation of non-linear valve law and ventricular interaction dynamics in the minimal cardiac model," Comput Methods Programs Biomed, Vol 80, pp. 65-74, 2005.

Smith, BW, Chase, JG, Shaw, GM and Nokes, RI. "Simulating transient ventricular interaction using a minimal cardiovascular system model," Physiol Meas, Vol 27, pp. 165-179, 2006.

Hann, CE, Chase, JG and Shaw, GM. "Integral-Based Identification of Patient Specific Parameters for a Minimal Cardiac Model," Computer Methods and Programs in Biomedicine, Vol 81(2), pp. 181-192, 2006.

Ghuysen, A. Lambermont, B. Kolh, P. Tchana-Sato, V., Magis, D. Gerard, P. Mommens, V. Janssen, N. Desaive T. and D'Orio, V. "Alteration of right ventricular-pulmonary vascular coupling in a porcine model of progressive pressure overloading," Shock, Vol 29(2), pp.197-204, 2008.

Ueda, H, Hayshi, T, Tsumura, K. et al. "Inflection point of ascending aortic waveform is a predictive factor for all cause cardiovascular mortality in patients with chronic renal failure on hemodialysis," Am J Hypertens, Vol 17, pp. 1151-1155, 2004.